

Revisiting the Chlorine Abundance in Diffuse Interstellar Clouds from Measurements with the *Copernicus* Satellite

Daniel Moomey¹, S. R. Federman¹, and Y. Sheffer^{1,2}

ABSTRACT

We reanalyzed interstellar Cl I and Cl II spectra acquired with the *Copernicus* satellite. The directions for this study come from those of Crenny & Federman and sample the transition from atomic to molecular rich clouds where the unique chemistry leading to molecules containing chlorine is initiated. Our profile syntheses relied on up-to-date laboratory oscillator strengths and component structures derived from published high-resolution measurements of K I absorption that were supplemented with Ca II and Na I D results. We obtain self-consistent results for the Cl I lines at 1088, 1097, and 1347 Å from which precise column densities are derived. The improved set of results reveals clearer correspondences with H₂ and total hydrogen column densities. These linear relationships arise from rapid conversion of Cl⁺ to Cl⁰ in regions where H₂ is present.

Subject headings: atomic data — ISM: abundances — ISM: — ultraviolet: ISM

1. Introduction

There is renewed interest in the elemental abundance of chlorine in diffuse interstellar clouds. Previous observations (Jura & York 1978; Harris & Bromage 1984; Jenkins et al. 1986) focused on the unique chemical property that, of the abundant elements, only the dominant ion of Cl, Cl⁺, has exothermic reactions with H₂, and equally important, they occur on nearly every collision. As a result, observations acquired with the *Copernicus* satellite and the *International Ultraviolet Explorer* (*IUE*) examined the relative amounts of Cl⁰ and Cl⁺ as a function of H₂ column, average line-of-sight density, etc. Jura & York (1978) examined *Copernicus* spectra for 10 sight lines and found that the interstellar chlorine

¹Department of Physics and Astronomy, University of Toledo, Toledo, OH 43606, USA; steven.federman@utoledo.edu

²Department of Astronomy, University of Maryland, College Park, MD 20742, USA; ysheffer@astro.umd.edu

abundance appeared to be relatively constant and that the results were consistent with their chemical model. This work was expanded to 40 directions by Harris & Bromage (1984), who relied on data for Cl I $\lambda\lambda 1097, 1347$ and Cl II $\lambda 1071$ acquired with the *Copernicus* satellite and compiled by Bohlin et al. (1983). These were supplemented with their own spectra of $\lambda 1347$ obtained with *IUE*. Harris & Bromage surmised that the chlorine abundance did not vary appreciably with distance to the background star nor with $E(B - V)$, but that the abundance decreased with increasing average gas density, $\langle n \rangle [N_{tot}(\text{H})/\text{distance to star}]$, where $N_{tot}(\text{H}) = N(\text{H I}) + 2 N(\text{H}_2)$. Their expanded sample continued to support the chemical model. As part of an analysis of interstellar abundances for several elements based on the data collected by Bohlin et al. (1983), Jenkins et al. (1986) found that the chlorine abundance varied with $\langle n \rangle$ through the use of detailed statistical arguments.

The more recent interest revolves around four issues. First, Sonnentrucker et al. (2002) described an analysis where the fraction of Cl in the neutral form provides information about the molecular hydrogen content of the gas. Second, detections of interstellar fluorine with the *Far Ultraviolet Spectroscopic Explorer (FUSE)* by Federman et al. (2005) and Snow, Destree, & Jensen (2007) were interpreted in part through comparison with the Cl abundance because both halogens are expected to have similar levels of depletion onto grains. Third, a self-consistent set of oscillator strengths (f -values) for lines of Cl I ($\lambda\lambda 1088, 1097$, and 1347) and Cl II ($\lambda 1071$) is now available based on laboratory experiments (Schechtman et al. 1993; 2005) and theoretical calculations (Biémont, Gebarowski, & Zeippen 1994; Tayal 2004; Froese Fischer, Tachiev, & Irimia 2006; Oliver & Hibbert 2007). Fourth, measurements with the *Herschel Space Observatory* (Lis et al. 2010) of H_2Cl^+ and HCl in absorption from diffuse molecular gas allows a more complete analysis of chlorine chemistry.

We used the improved set of oscillator strengths to reevaluate the chemical trends involving neutral and singly ionized chlorine with atomic and molecular hydrogen. The chlorine data come from the sight lines analyzed by Crenny & Federman (2004) for CO absorption. Since the f -value for the Cl II line at 1071 \AA has not changed significantly from the value adopted by Jenkins et al. (1986), as noted by Schechtman et al. (2005), we do not discuss the chlorine depletion patterns here. Instead, the use of the three Cl I lines, along with profile synthesis based on component structure for the line of sight from high-resolution ground-based measurements, provides the means to study the correspondences between the chlorine and hydrogen species with greater precision than was possible in the earlier work.

2. Observations

Earlier studies of Cl I derived column densities either by assuming an optically thin line ($\lambda 1097$) or through curves of growth that yielded an effective b -value consistent with the measured equivalent width (W_λ) for the line at 1347 \AA . An effective b -value arises when the component structure from individual clouds is not resolved. Our sample mainly comprises the directions from Crenny & Federman (2004) because Cl I $\lambda 1088$ is blended with the CO $C - X$ (0,0) band, which was the focus in that paper. Once the column density of CO was known, the absorption from the $C - X$ (0,0) band could be removed from the spectrum, leaving only $\lambda 1088$. The importance of this line lies in the fact that it has a strength intermediate between those for the lines at 1097 and 1347 \AA . To this sample, we added the observations on ρ Oph A and χ Oph, which were analyzed for CO absorption by Federman et al. (2003). Since chlorine depletion was not our focus, we did not include moderately reddened, molecule-rich directions such as o Per, ζ Per, and ζ Oph.

High-resolution spectra acquired with the U1 photomultiplier tube were extracted from the *Copernicus* archive at the Multiwavelength Archive at the Space Telescope Science Institute (MAST). The spectra, with a nominal resolution of 0.05 \AA , revealed absorption from Cl II $\lambda 1071$ and the three lines of Cl I at 1088, 1097, and 1347 \AA . The processing of the MAST data was essentially the same as that done on the CO data by Crenny & Federman (2004). Scans indicating stellar continua on both sides of the interstellar feature and free of peculiarities were rebinned and summed, resulting in a final spectrum for further analysis. Using standard routines in the IRAF environment, rectified spectra were obtained through low-order polynomial fits to the stellar continua. As with the data analyzed by Crenny & Federman (2004), all MAST spectra were corrected for particle background, but stray light and scattered light were not removed because accidental blockage of the stray-light source may have occurred and scattered light could represent only 5 to 10% of the local continuum. The consequences of not accounting for these effects can be assessed by comparison with results from earlier studies. This comparison of equivalent widths appears in Table 1. Our uncertainties were determined by multiplying the rms deviations in the rectified stellar continuum by the width of the interstellar feature at the 50% level. When no line was present, $3\text{-}\sigma$ upper limits were derived.

Our values of W_λ agree well with previous determinations (Jura & York 1978; Bohlin et al. 1983; Federman 1986) when the mutual uncertainties are considered. The occasional discrepancy involves measurements of W_{1088} between Federman (1986) and us, such as toward ϵ Per and π Sco. The differences can be ascribed to the difficulty in accounting for absorption from the CO $C - X$ (0,0) band; however, for most sight lines the two sets of results agree. An additional comparison of *Copernicus* data for $\lambda 1088$ is possible; toward γ Ara Morton &

Hu (1975) found 6.8 ± 0.7 mÅ versus our measurement of 6.3 ± 0.4 mÅ. Finally, the line at 1347 Å was observed toward several bright stars with grating G160M of the Goddard High Resolution Spectrograph on the *Hubble Space Telescope*: η Tau (21.8 ± 0.7 vs. 15.4 ± 3.1 mÅ), 1 Sco (27.9 ± 0.9 vs. 20.5 ± 4.8 mÅ), π Sco (15.8 ± 0.4 vs. 15.5 ± 1.3 mÅ), and σ Sco (21.2 ± 0.4 vs. 21.4 ± 4.3 mÅ). The correspondence is very good, within the $2\text{-}\sigma$ uncertainties of the *Copernicus* results in all cases. We believe, therefore, that the effects of stray light and scattered light do not impact our results in a significant way.

3. Results and Discussion

A further refinement in our analysis is the use of profile synthesis to extract column densities, taking into account known component structures. As in much of our previous syntheses, we utilized the fitting routine ISMOD (Sheffer, unpublished) with the laboratory f -values reported by Schectman et al. (1993, 2005). The component structure was inferred from published ground-based observations of K I (Welty & Hobbs 2001; Pan et al. 2004), Ca II (Vallerga et al. 1993; Welty, Morton, & Hobbs 1996; Welsh et al. 1997; Pan et al. 2004; Ritchey et al. 2006), and Na I D (Crawford, Barlow, & Blades 1989; Welsh et al. 1991; Welty, Hobbs, & Kulkarni 1994; White et al. 2001), all of which were acquired at spectral resolution much higher than that of the *Copernicus* measurements. Because the Na I D lines are usually severely optically thick, even in very diffuse sight lines, we treated these measurements as secondary. The first step was to check for consistency in component structure among independent studies for a specific species and from one species to the other. The correspondence was quite good. For the most part, we relied on the components seen in K I for velocities, but allowed the b -values and fractional column densities to vary. Occasionally, we had to combine nearby components, weighted according to component column density, in order to not overfit the observed absorption; this was necessary for the sight lines toward 139 Tau, 1 Sco, π Sco, ν Sco, χ Oph, and 59 Cyg. In a few cases, such as γ Ara, we did not consider absorption from a substantially weaker component. For HD 21278, α Cam, and 1 Cas, high-resolution component structure was not available, and so we fit absorption in the latter two directions with one or two components having b -values less than about 2 km s^{-1} (see e.g., Pan et al. 2005 for discussion of limits). For HD 21278, incorrect removal of CO absorption in the vicinity of $\lambda 1088$ and the lack of Cl II prevented us from deriving reliable results; this sight line is not considered in the analyses presented below.

Final column densities $[N(X)]$ were derived through the following steps. First, the Cl I lines were fit with the same component structure from the ground-based spectra. If any of the lines were overfit (as revealed by significantly less noise in the residuals within the range

of absorption compared to the continuum), fits with fewer components were attempted. The individual uncertainties in column density were inferred from the uncertainty in W_λ for the line. Once consistent column densities were obtained for the Cl I lines, a weighted average yielded our preferred value for $N(\text{Cl I})$. The same component structure was then used to fit the absorption from Cl II $\lambda 1071$. Figure 1 shows the results of the profile synthesis for the gas toward ϵ Per and σ Sco. The spectral ranges for $\lambda\lambda 1088, 1097$ shown for σ Sco were limited by the extent of the original scans.

Our column densities, along with those of earlier analyses of *Copernicus* spectra (Jura & York 1978; Harris & Bromage 1984; Jenkins et al. 1986) scaled to the oscillator strengths used here, appear in Table 2, and the values of W_λ from the fits are given in Table 1. Our measured W_λ s and the fitted values are in close agreement. As for the comparison of column densities, we first note that the results of Harris & Bromage (1984) in Table 2 were based in part on analysis of *IUE* spectra, which were not considered by us because they have lower spectral resolution and generally lower signal to noise. Moreover, the results of Jenkins et al. (1986) are based on the data compiled in Bohlin et al. (1983). Previous and our determinations agree for the most part, with ours having improved precision. This arises from our use of more than one line for Cl I and from the adoption of component structure from high-resolution spectra of K I, Ca II, and Na I D. It is also worth comparing the b -values deduced by Jenkins et al. (1986) with our component structure. For the sight lines with a single component (1 Sco, ν Sco, μ Nor, 59 Cyg, and 1 Cas), the b -values are very similar. For the other sight lines, the b -values from Jenkins et al. (1986) are larger than ours, but instead are consistent with the range in velocities for the components used in our study. In essence, the values quoted by Jenkins et al. (1986) for the latter group are effective b -values.

We examined the resulting trends among $N(\text{Cl I})$ and $N(\text{Cl II})$ with $N(\text{H I})$ and $N(\text{H}_2)$, as well as $N_{\text{tot}}(\text{Cl})$ [$N(\text{Cl I}) + N(\text{Cl II})$] versus $N_{\text{tot}}(\text{H})$. The hydrogen results come from Savage et al. (1977). For the sight lines in common, the values of $N(\text{H I})$ of Savage et al. agree with those of Diplas & Savage (1994), considering the uncertainties quoted (≈ 0.10 dex) by the latter authors. We, therefore, assigned uncertainties of 0.10 dex to $N(\text{H I})$ for our sample.

Only two relationships revealed significant trends, $N(\text{Cl I})$ vs. $N(\text{H}_2)$ and $N_{\text{tot}}(\text{Cl})$ vs. $N_{\text{tot}}(\text{H})$, and they are shown in Figures 2 and 3. [These two relationships had correlation coefficients (r^2) greater than 0.6, compared to ≤ 0.3 for the others.] Our BCES least-squares fits (Akritas & Bershady 1996), which allow the uncertainties in x and y to be treated independently, are also given. In Fig. 3, directions with limits on $N(\text{Cl II})$ or those without H I column densities are not included in the fits. The latter three points lie at least 1.0 dex to the left of the data shown here.

Figure 2 shows the relationship between neutral chlorine and molecular hydrogen. The data reveal a linear trend with a slope of 0.92 ± 0.19 that spans a range in column densities of nearly 100. The close correspondence between Cl^0 and H_2 arises from rapid hydrogen abstraction reactions between Cl^+ and H_2 and the subsequent dissociative recombination of the molecular ions and the photodissociation of HCl (e.g., Jura 1974; Lis et al. 2010). This figure provides a firm foundation for deriving the molecular hydrogen content from observations of neutral chlorine (Sonnentrucker et al. 2002).

Next we consider the trend seen in Figure 3, a plot of $\log N_{\text{tot}}(\text{Cl})$ vs. $\log N_{\text{tot}}(\text{H})$. The BCES fit again suggests a linear relationship, with a slope of 1.07 ± 0.14 . Most of the sight lines with upper limits to $N(\text{Cl II}) - \alpha$ Cam, 59 Cyg, and 1 Cas – are consistent with the fit, as is the result for 67 Oph, which has no spectrum of $\text{Cl II } \lambda 1071$. Only the diffuse gas toward ν Sco suggests the presence of an anomaly, but we note that the limited spectral coverage in the vicinity of $\lambda 1071$ might have compromised the result. Of the directions in our sample, only the sight line toward ρ Oph indicates depletion of chlorine onto grains. This is not unexpected because it has the largest $\langle n \rangle$. Thus, ρ Oph was excluded from the fit as well. A weighted average of the results for directions indicated by filled circles yields a chlorine abundance, $N_{\text{tot}}(\text{Cl})/N_{\text{tot}}(\text{H})$, of -6.99 ± 0.04 . Our inferred abundance compares favorably with previous determinations: -6.95 ± 0.03 (Harris & Bromage 1984) and -7.09 ± 0.03 (Jenkins et al. 1986). Both previous values have been scaled to reflect the revised f -value given by Schectman et al. (2005) for Cl II , whose absorption dominates the low-density sight lines considered by Harris & Bromage and Jenkins et al. When compared with the meteoritic abundance of -6.74 ± 0.06 (Lodders 2003), the interstellar gas phase abundance of chlorine indicates a factor of nearly two depletion onto grains.

At first glance, it may seem surprising that our sample of directions, which probe the transition from atomic to molecular gas, shows such a correspondence between $N_{\text{tot}}(\text{Cl})$ and $N_{\text{tot}}(\text{H})$ and a chlorine abundance indistinguishable from earlier determinations. Our sample includes some sight lines where most of the Cl is singly-ionized, while others are dominated by neutral chlorine. Moreover, the average densities for the gas toward our targets range between $\langle n \rangle$ of 0.25 cm^{-3} and 6 cm^{-3} , except for gas toward ρ Oph, which has $\langle n \rangle$ greater than 10 cm^{-3} . Usually, interstellar abundances are inferred from results for sight lines with $\langle n \rangle$ less than about 0.1 cm^{-3} (e.g., Jenkins et al. 1986). We suggest that the difference with results for other elements discussed by Jenkins et al. (1986) – Mg, P, Mn, and Fe – and by Ritchey et al. (2011) – B, O, Cu, and Ga, for instance, again is connected to the rapid reactions between Cl^+ and H_2 , resulting in conversion of Cl^+ to Cl^0 that occurs on time scales that are short compared to those associated with depletion onto grains. Based on the rate coefficient for $\text{Cl}^+ + \text{H}_2 \rightarrow \text{HCl}^+ + \text{H}$, the initial reaction in the sequence, given by Anicich (1993) and a density of 1 cm^{-3} , we obtain a rate of about 10^{-9} s^{-1} , or a time

scale of about 30 years. Other reactions in the sequence are equally fast. We also note that the range in $N(\text{Cl II})/N(\text{Cl I})$ ratios found for our sample is the likely cause for the weak correlation between Cl^+ and atomic H.

As noted in the introduction, we undertook this study in part because a self-consistent set of f -values was emerging for the Cl I lines commonly studied in diffuse clouds, $\lambda\lambda 1088$, 1097, and 1347. This came about in part through the realization that energy levels required new identifications (Biémont et al. 1994; Oliver & Hibbert 2007). However, other lines are seen in interstellar spectra. Sonnentrucker, Friedman, & York (2006) used the results of Schectman et al. (1993) as a starting point in deriving f -values for relatively weak Cl I lines at 1004, 1079, 1090, and 1094 Å seen in spectra acquired with *FUSE*. These lines are especially useful for more reddened directions. Here, the correspondence between empirical measures and theoretical calculations of Biémont et al. (1994) is less satisfactory, while that for the results of Oliver & Hibbert (2007) for $\lambda 1094$ is good. Their reevaluation of assigning term values to a number of energy levels probably led to the improvement.

Lis et al. (2010) detected absorption from H_2Cl^+ and HCl in diffuse molecular clouds along the line of sight toward the star-forming region Sgr B2(S). They derived a combined abundance for these chlorine molecules of about 4×10^{-9} , which is about 1% of the total chlorine budget (see above). The remainder is likely in atomic forms and depleted onto interstellar grains. This is consistent with the tentative detection of HCl absorption at UV wavelengths seen toward ζ Oph (Federman et al. 1995). Furthermore, the $\text{HCl}/\text{H}_2\text{Cl}^+$ ratio derived by Lis et al. (2010), about 1, agrees with expectations from modeling diffuse clouds.

4. Conclusions

We reanalyzed a sample of directions that were observed with the *Copernicus* satellite and that involve diffuse clouds where the transition from atomic to molecular gas takes place. The basis for the sample comes from the work of Crenny & Federman (2004), who studied CO absorption, but our focus was on data for lines of Cl I and Cl II. Column densities were extracted from profile syntheses that relied on up-to-date oscillator strengths and component structures from higher resolution, ground-based observations. The result is the most precisely determined set of column densities for our sample to date. We examined the correspondence between $N(\text{Cl I})$ and $N(\text{H}_2)$ and between $N_{\text{tot}}(\text{Cl})$ and $N_{\text{tot}}(\text{H})$ and found strong linear trends in both cases. We attributed the trends to the rare instance of a rapid ion-molecule reaction between a singly ionized atom, Cl^+ , and H_2 . Our findings are likely to aid in interpreting observations of HCl and H_2Cl^+ absorption from diffuse clouds revealed by *Herschel*.

This work was supported by NASA grant NNG 06-GC70G. We acknowledge the assistance provided by Michael Stone in the early phases of the research reported here and the helpful exchanges with Don York, Ed Jenkins, and Jim Lauroesch regarding the background in *Copernicus* spectra. We utilized the *Copernicus* archive available at the Multiwavelength Archive at the Space Telescope Science Institute. Additional observations made with the NASA/ESA Hubble Space Telescope were obtained from the data archive at STScI. STScI is operated by the Association of Universities for Research in Astronomy, Inc. under NASA contract NAS5-26555.

REFERENCES

- Anicich, V.G. 1993, J. Phys. Chem. Ref. Data, 22, 1469
- Akritas, M.G., & Bershadsky, M.A. 1996, ApJ, 470, 706
- Biémont, E., Gebarowski, R., & Zeippen, C.J. 1994, A&A, 287, 290
- Bohlin, R.C., Jenkins, E.B., Spitzer, L., York, D.G., Hill, J.K., Savage, B.D., & Snow, T.P. 1983, ApJS, 51, 277
- Crawford, I.A., Barlow, M.J., & Blades, J.C. 1989, ApJ, 336, 212
- Crenny, T., & Federman, S.R. 2004, ApJ, 605, 278
- Diplas, A., & Savage, B.D. 1994, ApJS, 93, 211
- Federman, S.R. 1986, ApJ, 309, 306
- Federman, S.R., Cardell, J.A., van Dishoeck, E.F., Lambert, D.L., & Black, J.H. 1995, ApJ, 445, 325
- Federman, S.R., Lambert, D.L., Sheffer, Y., Cardelli, J.A., Andersson, B.-G., van Dishoeck, E.F., & Zsargó, J. 2003, ApJ, 591, 986
- Federman, S.R., Sheffer, Y., Lambert, D.L., & Smith, V.V. 2005, ApJ, 619, 884
- Froese Fischer, C., Tachiev, G., & Irimia, A. 2006, At. Data Nucl. Data Tables, 92, 607
- Harris, A.W., & Bromage, G.E. 1984, MNRAS, 208, 941
- Jenkins, E.B., Savage, B.D., & Spitzer, L. 1986, ApJ, 301, 355
- Jura, M. 1974, ApJ, 190, L33

- Jura, M., & York, D.G. 1978, *ApJ*, 219, 861
- Lis, D.C. et al. 2010, *A&A*, 521, L9
- Lodders, K. 2003, *ApJ*, 591, 1220
- Morton, D.C., & Hu, E.M. 1975, *ApJ*, 202, 638
- Oliver, P., & Hibbert, A. 2007, *J. Phys. B*, 40, 2847
- Pan, K., Federman, S.R., Cunha, K., Smith, V.V. & Welty, D.E. 2004, *ApJS*, 151, 313
- Pan, K., Federman, S.R., Sheffer, Y., & Andersson, B.-G. 2005, *ApJ*, 633, 986
- Ritchey, A.M., Federman, S.R., Sheffer, Y., & Lambert, D.L. 2011, *ApJ*, 728, 70
- Ritchey, A.M., Martinez, M., Pan, K., Federman, S.R., & Lambert, D.L. 2006, *ApJ*, 649, 788
- Savage, B.D., Bohlin, R.C., Drake, J.F., & Budich, W. 1977, *ApJ*, 216, 291
- Schectman, R.M., Federman, S.R., Beideck, D.J., & Ellis, D.G. 1993, *ApJ*, 406, 735
- Schectman, R.M., Federman, S.R., Brown, M., Cheng, S., Fritts, M.C., Irving, R.E., & Gibson, N.D. 2005, *ApJ*, 621, 1159
- Snow, T.P., Destree, J.D., & Jensen, A.G. 2007, *ApJ*, 655, 285
- Sonnentrucker, P., Friedman, S.D., Welty, D.E., York, D.G., & Snow, T.P. 2002, 576, 241
- Sonnentrucker, P., Friedman, S.D., & York, D.G. 2006, *ApJ*, 650, L115
- Tayal, S.S. 2004, *A&A*, 426, 717
- Vallerga, J.V., Vedder, P.W., Craig, N., & Welsh, B.Y. 1993, *ApJ*, 411, 729
- Welsh, B.Y., Sasseen, T., Craig, N., Jelinsky, S., & Albert, C.E. 1997, *ApJS*, 112, 507
- Welsh, B.Y., Vedder, P.W., Vallerga, J.V., & Craig, N. 1991, *ApJ*, 381, 462
- Welty, D.E. & Hobbs, L.M. 2001, *ApJS*, 133, 345
- Welty, D.E., Hobbs, L.M., & Kulkarni, V.P. 1994, *ApJ*, 436, 152
- Welty, D.E., Morton, D.C., & Hobbs, L.M. 1996, *ApJS*, 106, 533

White, R.E., Allen, C.L., Forrester, W.B., Gonnella, A.M., & Young, K.L. 2001, ApJS, 132, 253

Table 1. Comparison of Equivalent Widths (in mÅ)

Star	Name	Line (Å) ^a	This Work	JY ^b	BJSYHSS ^c	F ^d	Fit
HD 23408	20 Tau	1071	≤6.8	...	15.0±15.3	...	≤2.0
		1088	23.5±5.2	14.9
		1097	≤35.6	3.0
		1347	22.2±10.3	...	11.3±15.1	...	24.5
HD 23630	η Tau	1071	≤6.9	...	−3.0±18.3	...	≤2.1
		1088	≤4.3	3±2	11.3
		1097	3.7±1.7	2.8
		1347	15.4±3.1	...	25.4±7.4	...	17.6
HD 24760	ε Per	1071	2.7±0.7	3.0±1	2.3±0.6	...	2.8
		1088	8.1±0.4	15±2	7.9
		1097	0.9±0.2	2.5±0.7	1.0
		1347	21.4±0.6	22±2	22.5±1.4	...	18.9
HD 30614	α Cam	1071	≤3.6	15±6	11.4±4.9	...	≤1.0
		1088	37.4±3.1	23±2	37.0
		1097	9.4±1.8	11±4	16.2±3.1	...	10.3
		1347	20.5±4.8	...	29.6±6.3	...	18.5
HD 36861	λ Ori	1071	5.9±1.3	7±1	7.8±1.0	...	6.0
		1088	10.9±0.9	10±1	11.2
		1097	3.0±0.9	3±1	1.7
		1347	27.8±2.2	...	33.3±5.3	...	28.8
HD 40111	139 Tau	1071	8.4±2.4	...	12.5±2.3	...	10.2
		1088	8.2±1.0	11.4
		1097	≤2.6	...	1.4±2.0	...	1.4
		1347	27.8±2.2	...	33.3±5.3	...	28.8
HD 141637	1 Sco	1071	9.0±4.4	...	17.3±5.9	...	9.6
		1088	5.4±1.2	7.5
		1097	≤3.1	...	3.0±2.0	...	0.9
		1347	20.5±4.8	...	29.6±6.3	...	18.5
HD 143018	π Sco	1071	7.4±2.2	6.4
		1088	4.8±0.2	8±1	5.2
		1097	≤0.5	0.6
		1347	15.5±1.3	13.0
HD 143275	δ Sco	1071	10.8±0.2	...	10.9±0.4	...	10.1
		1088	16.1±1.0	18±1	15.4
		1097	4.2±0.3	...	3.1±0.4	...	3.1
		1347	20.5±4.8	...	29.6±6.3	...	18.5
HD 144217	β ¹ Sco	1071	8.4±0.2	...	9.8±0.8	...	9.0
		1088	18.9±0.4	19.0
		1097	4.4±0.4	...	4.9±0.7	...	5.1
		1347	26.9±6.1	...	36.5±14.8	...	27.0
HD 144470	ω ¹ Sco	1071	14.9±3.9	...	16.3±1.8	...	14.8
		1088	17.7±1.4	23±6	18.0
		1097	3.0±1.0	...	3.4±1.7	...	3.6
		1347	26.9±6.1	...	36.5±14.8	...	27.0
HD 145502	ν Sco	1071	≤6.3	...	8.1±7.6	...	≤1.4
		1088	10.5±0.9	15±2	12.8
		1097	≤7.4	...	13.7±8.0	...	1.8
		1347	26.9±6.1	...	36.5±14.8	...	27.0

Table 1—Continued

Star	Name	Line (Å) ^a	This Work	JY ^b	BJSYHSS ^c	F ^d	Fit
HD 147165	σ Sco	1071	21.7±4.2	...	21.5±2.6	...	20.4
		1088	11.9±0.5	12.0
		1097	0.7±0.3	...	7.9±2.9	...	1.7
		1347	21.4±2.0	...	23.1±2.9	...	25.4
HD 147933	ρ Oph A	1071	7.1±2.3	...	15.6±4.6	...	7.1
		1088	17.2±2.4	29±7	14.8
		1097	3.1±0.8	...	8.3±4.0	...	3.0
		1347	20.5±4.3	...	22.7±9.1	...	24.9
HD 148184	χ Oph	1071	5.3±1.1	...	8.3±4.5	...	5.5
		1088	16.1±2.5	26.0
		1097	10.9±2.3	...	14.4±3.6	...	11.4
		1347	39.2±7.0	...	42.4±6.6	...	37.4
HD 149038	μ Nor	1071	8.4±3.0	...	61.6±25.6	...	8.0
		1088	33.0±2.4	36 ⁺¹⁶ ₋₉	34.0
		1097	20.4±3.6	...	3.5±15.8	...	12.2
		1347	18.9±0.9	22±6	23.5±1.5	...	18.8
HD 157246	γ Ara	1071	15.4±1.5	9±2	20.9±1.3	...	12.3
		1088	6.3±0.4	7.1
		1097	2.1±0.7	2.5±1.4	0.8
		1347	18.9±0.9	22±6	23.5±1.5	...	18.8
HD 164353	67 Oph	1088	23.6±3.5	11 ⁺⁷ ₋₆	19.9
HD 200120	59 Cyg	1071	≤3.1	...	2.7±2.8	...	≤1.9
		1088	2.5±0.9	6±2	3.4
		1097	4.4±1.6	...	0.8±2.6	...	0.5
		1347	8.3±3.2	...	15.9±4.6	...	7.7
HD 217675	o And	1071	1.0±9.4	...	^e
		1088	11.9±1.4	14±2	10.8
		1347	21.7±2.7	...	25.9±6.1	...	23.1
HD 218376	1 Cas	1071	≤14.7	...	10.3±5.1	...	≤6.6
		1088	18.3±9.6	21.9
		1097	6.5±2.0	...	12.7±4.5	...	7.2

^aThe entries refer to Cl II λ 1071; Cl I $\lambda\lambda$ 1088, 1097, 1347.

^bJura & York 1978.

^cBohlin et al. 1983.

^dFederman 1986.

^eThis line is severely blended with absorption from H₂.

Table 2. Column Densities

Star	$N(\text{Cl II})^{\text{a}}$	$N(\text{Cl I})^{\text{a}}$	$N_{\text{tot}}(\text{Cl})^{\text{a}}$	$\log N(\text{H I})^{\text{b}}$	$\log N(\text{H}_2)^{\text{b}}$	$\log N_{\text{tot}}(\text{H})^{\text{b}}$
20 Tau	≤ 1.4 11.0(0.0-129) ^{c, d}	3.5 ± 0.8 0.9(0.5-3.7) ^c	≤ 4.9	...	19.75	≥ 20.05
η Tau	≤ 1.5	3.4 ± 0.6 1.3(0.4-sat.) ^c	≤ 4.9	...	19.54	≥ 19.84
ϵ Per	1.9 ± 0.5 1.4(0.6-2.4) ^c 1.9(1.2-2.3) ^e 1.4(1.0-1.8) ^f	1.1 ± 0.1 1.3(1.0-2.2) ^c 1.8(1.2-3.0) ^e 1.0(0.9-1.1) ^f	3.0 ± 0.5	20.40	19.53	20.50
α Cam	≤ 2.5 7.8(0.9-16.2) ^c 9.3(5.9-11.7) ^e 7.1(4.0-10.0) ^f	13.0 ± 1.0 20.0(8.9-35.6) ^c 11.8(7.4-18.7) ^e 17.5(13.8-20.5) ^f	≤ 15.5	20.90	20.34	21.09
λ Ori	4.7 ± 1.0 5.1(3.7-6.9) ^c 4.4(3.5-5.5) ^e 4.8(4.2-5.5) ^f	1.9 ± 0.2 1.2(0.9-1.6) ^c 3.2(2.0-4.0) ^e 1.1(1.0-1.2) ^f	6.6 ± 1.0	20.78	19.11	20.80
139 Tau	7.4 ± 2.1 7.8(0.9-16.2) ^c 7.8(6.3-9.1) ^f	1.5 ± 0.1 3.6(1.7-7.1) ^c 1.6(1.3-2.0) ^f	8.9 ± 2.1	20.90	19.74	20.96
1 Sco	7.5 ± 3.7 8.7(5.2-13.2) ^c 10.7(7.1-14.4) ^f	1.0 ± 0.1 3.2(1.3-11.2) ^c 1.4(1.0-1.8) ^f	8.5 ± 3.7	21.19	19.23	21.20
π Sco	4.9 ± 1.5	0.70 ± 0.03	5.6 ± 1.5	20.72	19.32	20.75
δ Sco	9.9 ± 0.2 7.6(6.8-8.5) ^c 6.8(6.5-7.1) ^f	3.7 ± 0.2 3.6(2.8-4.5) ^c 3.3(2.9-3.7) ^f	13.6 ± 0.3	21.15	19.41	21.16
β^1 Sco	8.4 ± 0.2 6.6(5.5-7.9) ^c 6.0(5.6-6.6) ^f	6.5 ± 0.1 6.3(4.5-8.0) ^c 5.3(4.5-5.9) ^f	14.9 ± 0.3	21.09	19.83	21.14
ω^1 Sco	16.0 ± 4.0 11.7(8.7-16.2) ^c 10.0(8.9-11.2) ^f	4.2 ± 0.3 5.0(3.2-8.9) ^c 3.6(1.8-5.4) ^f	20.2 ± 4.0	21.18	20.05	21.24
ν Sco	≤ 1.0 4.7(0.0-26.9) ^c	2.0 ± 0.2 20.0(0.0-sat.) ^c	≤ 3.0	21.15	19.89	21.19
σ Sco	25.0 ± 5.0 17.8(12.0-28.2) ^c 13.2(11.7-14.8) ^f	1.9 ± 0.1 11.2(0.8-sat.) ^c 8.3(5.3-11.5) ^f	26.9 ± 5.0	21.34	19.79	21.37
ρ Oph A	6.0 ± 1.9 6.6(5.5-7.9) ^c 9.8(6.8-12.6) ^f	3.5 ± 0.4 6.3(4.5-8.0) ^c 8.9(4.6-18.6) ^f	9.5 ± 1.9	21.81	20.57	21.86
χ Oph	4.2 ± 0.9 11.7(8.7-16.2) ^c 5.1(2.3-7.9) ^f	18.0 ± 1.0 5.0(3.2-8.9) ^c 15.2(11.5-19.1) ^f	22.2 ± 1.2	21.15	20.63	21.35
μ Nor	6.2 ± 2.2 5.8(0.0-26.9) ^c 38.0(22.4-53.7) ^f	17.0 ± 1.0 20.0(0.8-sat.) ^c 13.2(9.4-21.9) ^f	23.2 ± 1.7	21.00	20.44	21.19

Table 2—Continued

Star	$N(\text{Cl II})^a$	$N(\text{Cl I})^a$	$N_{tot}(\text{Cl})^a$	$\log N(\text{H I})^b$	$\log N(\text{H}_2)^b$	$\log N_{tot}(\text{H})^b$
γ Ara	9.2 \pm 0.9 18.2(14.1-22.9) ^c 5.6(4.5-7.1) ^e 12.9(12.0-13.8) ^f	0.90 \pm 0.04 1.3(1.0-1.6) ^c 2.6(1.3-4.2) ^e 1.1(1.0-1.2) ^f	10.1 \pm 0.9	20.68	19.24	20.71
67 Oph	...	3.4 \pm 0.5	\geq 3.4	21.00	20.26	21.14
59 Cyg	\leq 2.5 1.7(0.0-6.5) ^c	0.50 \pm 0.12 1.4(0.4-sat.) ^c	\leq 3.0	20.26	19.32	20.34
σ And	...	1.5 \pm 0.1 1.8(0.6-sat.) ^c	\geq 1.5	...	19.67	\geq 19.97
1 Cas	\leq 5.4 2.2(0.0-5.4) ^c 6.3(3.2-9.5) ^f	9.6 \pm 2.6 7.1(4.0-14.1) ^c 13.5(8.7-18.3) ^f	\leq 15.0	20.95	20.15	21.07

^aPresent results given in first row; other determinations appear in subsequent rows. The column densities have units of 10^{13} cm^{-2} .

^bHydrogen results from Savage et al. 1977.

^cJenkins et al. 1986.

^dThe values in parentheses indicate quoted range in column density. ‘sat.’ indicates upper limits greatly affected by optical depth.

^eJura & York 1978.

^fHarris & Bromage 1984.

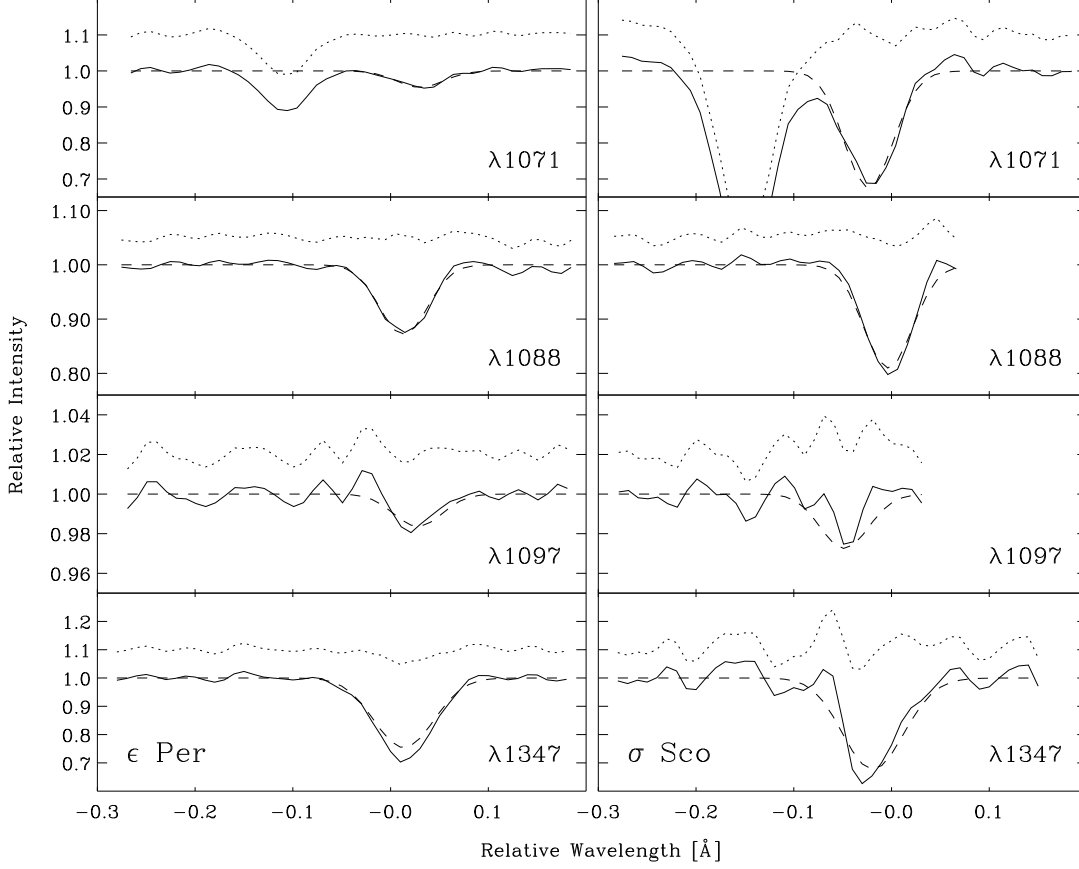


Fig. 1.— Sample spectra of Cl II and Cl I lines toward ϵ Per and σ Sco. Vertical scales from panel to panel vary. Absorption from H_2 is seen to the blue of Cl II $\lambda 1071$. Data are shown as solid lines, fits based on the weighted average Cl I column densities by dashed lines, and residuals by dotted lines. The slight offset in relative wavelength results from the accuracy of the original wavelength scale.

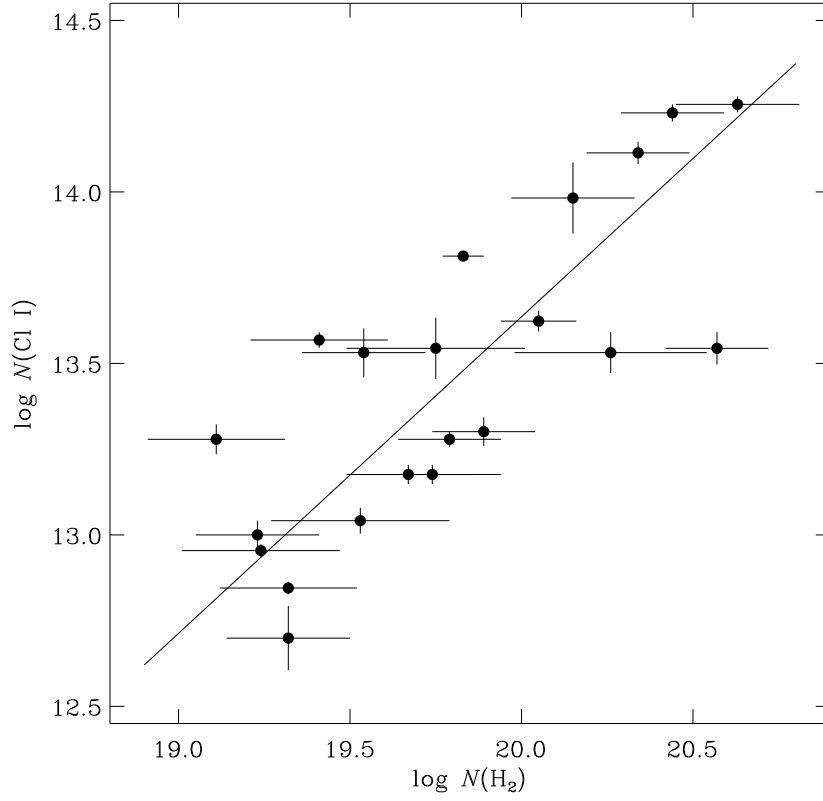


Fig. 2.— $\log N(\text{Cl I})$ vs. $\log N(\text{H}_2)$. Displayed uncertainties are 1σ . The linear fit is based on treating uncertainties in x and y independently. The resulting slope is 0.92 ± 0.19 .

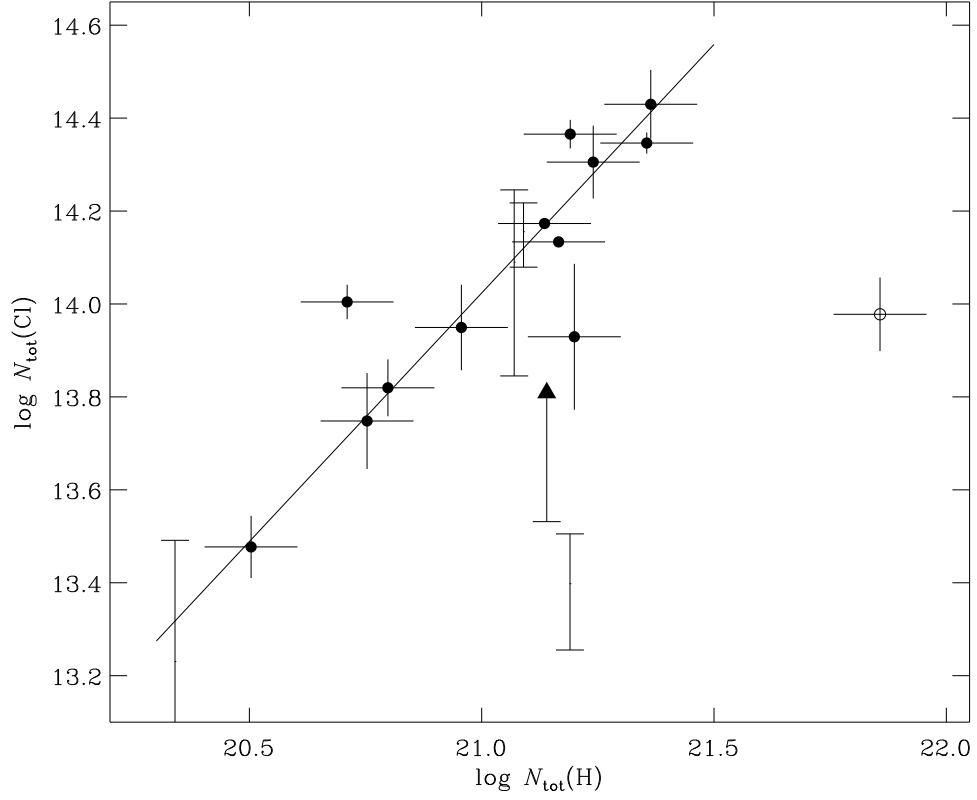


Fig. 3.— $\log N_{\text{tot}}(\text{Cl})$ vs. $\log N_{\text{tot}}(\text{H})$. Uncertainties are 1σ . Vertical lines with endcaps indicate directions with upper limits to $N(\text{Cl II})$, while the vertical arrow represents gas toward 67 Oph for which no Cl II spectrum is available. The result for ρ Oph is shown as an open circle. Sight lines without measures of $N(\text{H I})$ lie at least 1 dex to the left of the data shown here. A BCES linear fit to the filled circles yields a slope of 1.07 ± 0.14 .